Airborne validation of cirrus cloud properties derived from CALIPSO lidar measurements: Spatial properties

John E. Yorks,[1,2] Dennis L. Hlavka,[1,2] Mark A. Vaughan,[3] Matthew J. McGill,[2] William D. Hart,[1,2] Sharon Rodier,[1,3] and Ralph Kuehn[4]

[1] The Cloud-Aerosol Lidar Infrared Pathfinder Satellite Observations (CALIPSO) satellite was successfully launched in 2006 and has provided an unprecedented opportunity to study cloud and aerosol layers using range-resolved laser remote sensing. Dedicated validation flights were conducted using the airborne Cloud Physics Lidar (CPL) to validate the CALIPSO Level 1 and 2 data products. This paper presents results from coincident CALIPSO and CPL measurements of ice cloud spatial properties. Flight segment case studies are shown as well as statistics for all coincident measurements during the CALIPSO-CloudSat Validation Experiment (CC-VEX). CALIPSO layer detection algorithms for cirrus clouds are reliable in comparison with CPL, with best agreement occurring during nighttime coincident segments when the signal-to-noise ratio (SNR) of both instruments is greatest. However, the two instruments disagree on ice cloud spatial properties in two distinct cases. CALIPSO experiences less sensitivity to optically thin cirrus due to lower SNR when compared to CPL data at identical spatial scales. The incorporation of extended spatial averaging in the CALIPSO layer detection algorithm succeeds in detecting the optically thin cirrus, but the averaging process occasionally results in spatial smearing, both horizontally and vertically, of broken cirrus clouds. The second disparity occurs because, in contrast to CPL, multiple scattering contributes significantly to CALIPSO lidar measurements of cirrus clouds. As a result, the CALIPSO signal penetrates deeper into opaque cirrus clouds, and in these cases CALIPSO will report lower apparent cloud base altitudes than CPL.

Citation: Yorks, J. E., D. L. Hlavka, M. A. Vaughan, M. J. McGill, W. D. Hart, S. Rodier, and R. Kuehn (2011), Airborne validation of cirrus cloud properties derived from CALIPSO lidar measurements: Spatial properties, *J. Geophys. Res.*, *116*, D19207, doi:10.1029/2011JD015942.

1. Introduction

[2] The successful launch of the Cloud-Aerosol Lidar Infrared Pathfinder Satellite Observations (CALIPSO) [*Winker et al.*, 2007, 2009] satellite in April 2006 has provided the science community a five year global data set of vertical profiles of the spatial and optical properties of clouds and aerosols in the Earth's atmosphere. The primary payload aboard CALIPSO is the Cloud-Aerosol Lidar with Orthogonal Polarization (CALIOP), a dual wavelength, polarization-sensitive backscatter lidar [*Hunt et al.*, 2009]. The CALIOP data products have a large range of applications to significant climate system studies. For example, global cloud statistics have been compiled using collocated CALIOP and CloudSat data [*Sassen et al.*, 2008; *Haladay and Stephens*, 2009; *Mace et al.*, 2009] and collocated CALIOP and MODIS data [*Hu et al.*, 2007]. Cloud-aerosol interactions and radiative effects have been explored with CALIOP and CERES data [*Chand et al.*, 2009; *Yorks et al.*, 2009; *Costantino and Bréon*, 2010]. CALIOP data has been employed with forecast and general circulation models to study cloud statistics [*Chepfer et al.*, 2010; *Ahlgrimm and Köhler*, 2010; *Naud et al.*, 2010]. These studies included analysis of spatial properties of clouds and aerosols using CALIOP level 2 data products. The validation of these data products is thus crucial in quantifying uncertainties and detecting biases in the CALIOP retrievals and should in turn strengthen the results of previous and future studies using CALIOP data.

[3] The Cloud Physics Lidar (CPL) [*McGill et al.*, 2002] is an elastic backscatter lidar system operating at 1064, 532, and 355 nm, with depolarization resolved using the 1064 nm channel. Cloud spatial and optical properties are retrieved using the 1064 and 532 nm channels [*McGill et al.*, 2003]. Similar to CALIOP data, CPL data products have a wide-range of applications including the analysis of cloud properties [*McGill et al.*, 2003; *Bucholtz et al.*, 2010; *Davis et al.*, 2010] and the validation of satellite retrievals [*McGill et al.*,

---

[1]Science Systems and Applications, Inc., Lanham, Maryland, USA.
[2]NASA Goddard Space Flight Center, Greenbelt, Maryland, USA.
[3]NASA Langley Research Center, Hampton, Virginia, USA.
[4]Cooperative Institute for Meteorological Satellite Studies, University of Wisconsin-Madison, Madison, Wisconsin, USA.

Table 1. Fundamental Differences Between CPL and CALIOP

Parameter	CPL	CALIOP
Laser Repetition Rate	5.0 kHz	20.16 Hz
Laser Pulse Energy (532 nm)	25 μJ	110 mJ
Vertical Resolution at 10 km	30 m	60 m
Horizontal Resolution at 10 km	200 m	1 km
Platform Speed (m/s)	~200	~7500
Detection	Photon counting	analog
Receiver footprint at 10 km	1 m diameter	87 m diameter
Receiver FOV	100 urad	130 urad
Depolarization channel	1064 nm	532 nm

2007; *Ackerman et al.*, 2008]. The CPL is typically employed on the high-altitude NASA ER-2 aircraft, which flies above 20 km altitude. Therefore, the CPL provides "satellite-like" measurements from above the tropopause with higher SNR, higher resolution (both vertical and horizontal) and lower multiple scattering relative to space-based counterparts such as CALIOP. These characteristics make the CPL an ideal platform for validation of CALIOP data products. *McGill et al.* [2007] investigate the CALIOP version 1 calibrated backscatter profiles and assesses layer detection for specific case studies using CPL data. In this study, we analyze the spatial properties of cirrus clouds from version 3 level 2 CALIPSO cloud layer products to determine how the CALIPSO layer detection performs in comparison with CPL data on identical spatial scales, identify the differences between the cirrus cloud areas retrieved by the two instruments, and resolve the frequency and origin of these differences.

[4] To accommodate limits on telemetry bandwidth, the CALIOP data is averaged prior to downlink using a range-dependent on-board averaging scheme [*Winker et al.*, 2009]. As a result, the maximum spatial resolution of the CALIOP backscatter profiles in the upper troposphere (8.2 km to 20.2 km) is 1 km horizontally and 60 m vertically. During July and August in the northern hemisphere midlatitudes, the lower boundary of the altitude regime where cirrus clouds are expected is typically above 8 km. Furthermore, since the layer discrimination and multiple scattering corrections for both instruments are most reliable for cirrus clouds, only cloud layers above 8 km are analyzed in this study.

2. Similarities and Differences Between CALIOP and CPL

[5] There are several fundamental similarities and differences between the CALIOP and CPL systems that have a large impact in comparing spatial properties retrieved by the two instruments. Both CPL and CALIOP fundamentally measure range-resolved backscatter profiles of the Earth's atmosphere [*McGill et al.*, 2002; *Powell et al.*, 2009]. Thus, "apples-to-apples" comparisons can be performed for measurements over the full extent of the troposphere to the limit of signal attenuation. A similar calibration method is also employed for both instruments at 532 nm, as described by *McGill et al.* [2007]. Table 1 summarizes the hardware specifications of the two instruments. The CALIOP field-of-view (FOV) is larger than CPL. Also, CALIPSO has an orbital height of about 705 km, much higher than the typical ER-2 altitude of 20 km, giving CALIOP a greater distance from atmospheric features. Consequently, the CALIOP foot-

print at 10 km (87 m in diameter) is larger than CPL (1 m in diameter). These differences produce significant dissimilarities in the signal-to-noise ratio (SNR) and multiple scattering effects of the two instruments, which are unavoidable given the space-based nature of the CALIOP system.

[6] The accuracy with which a lidar can derive spatial and optical properties of clouds depends on its SNR. The SNR of CALIOP is much lower than that of CPL, with the differences attributed to the larger distance of the instrument from atmospheric features (~695 km versus 10 km) combined with laser pulse repetition frequency differences and limitations in laser pulse energy by the available electrical power [*Hunt et al.*, 2009; *Winker et al.*, 2009]. The individual profiles reported in the standard CPL data products have a horizontal resolution of about 200 m and are obtained by accumulating 5,000 consecutive laser pulses. At 532 nm and resolutions of 5 km horizontal and 60 m vertical, the CPL SNR is an order of magnitude greater than the CALIOP SNR at 12 km for nighttime clear sky conditions, based on a conservative estimate of the CALIOP SNR using results from *Hunt et al.* [2009] and CPL SNR derived from data presented in this paper. Furthermore, lidar SNR is degraded by operation during daytime hours, when optically thin cloud layers are difficult to distinguish from the noise due to high solar background from many sky scenes, especially dense water clouds, ice, or snow covered surfaces [*Young and Vaughan*, 2009]. For CALIOP, the consequences of this lower SNR include less accurate characterization of cloud phase using depolarization ratio [*Hu et al.*, 2009] and higher CALIOP minimum detectable backscatter for optically thin cirrus clouds in comparison to CPL [*McGill et al.*, 2007]. The latter can inhibit the CALIOP layer detection algorithm from distinguishing optically thin cirrus clouds from the signal noise.

[7] The usual method of increasing the SNR in a lidar system is to spatially average numerous profiles (i.e., pulse accumulation), especially to retrieve spatial and optical properties of weakly scattering layers. Consequently, the CALIOP data products are provided at various spatial resolutions and a multiscale layer detection method was developed to mitigate the impact of the lower SNR [*Vaughan et al.*, 2009]. However, for inhomogeneous or broken cloud fields, improving SNR by averaging the lidar signal can result in profiles producing results that are not representative of the spatial and optical properties of the atmospheric scene [*Winker et al.*, 2009]. An example of this phenomenon is shown in the attenuated total backscatter (km^{-1} sr^{-1}) image (Figure 1a) using CPL data from 26 July 2006. For each 30 m height bin, the total number of bins detecting a cloud in a given segment was divided by the total number of observed bins to provide vertical profiles of cloud area frequencies, shown for this segment in Figure 1b for spatial resolutions of 200 m and 5 km. A broken cirrus cloud field observed in the standard 200 m attenuated total backscatter (km^{-1} sr^{-1}) image (Figure 1a) and corresponding cloud area frequency (Figure 1b, dashed) has been averaged into a homogeneous cirrus layer at a resolution of 5 km (Figure 1b, solid), leading to cloud area frequencies as much as 25% higher in 5 km data. Extensive spatial averaging is required to produce CALIOP SNRs comparable to that of CPL. Given this averaging and the high ground speed at which CALIPSO passes through the atmospheric scene, it is difficult to accurately
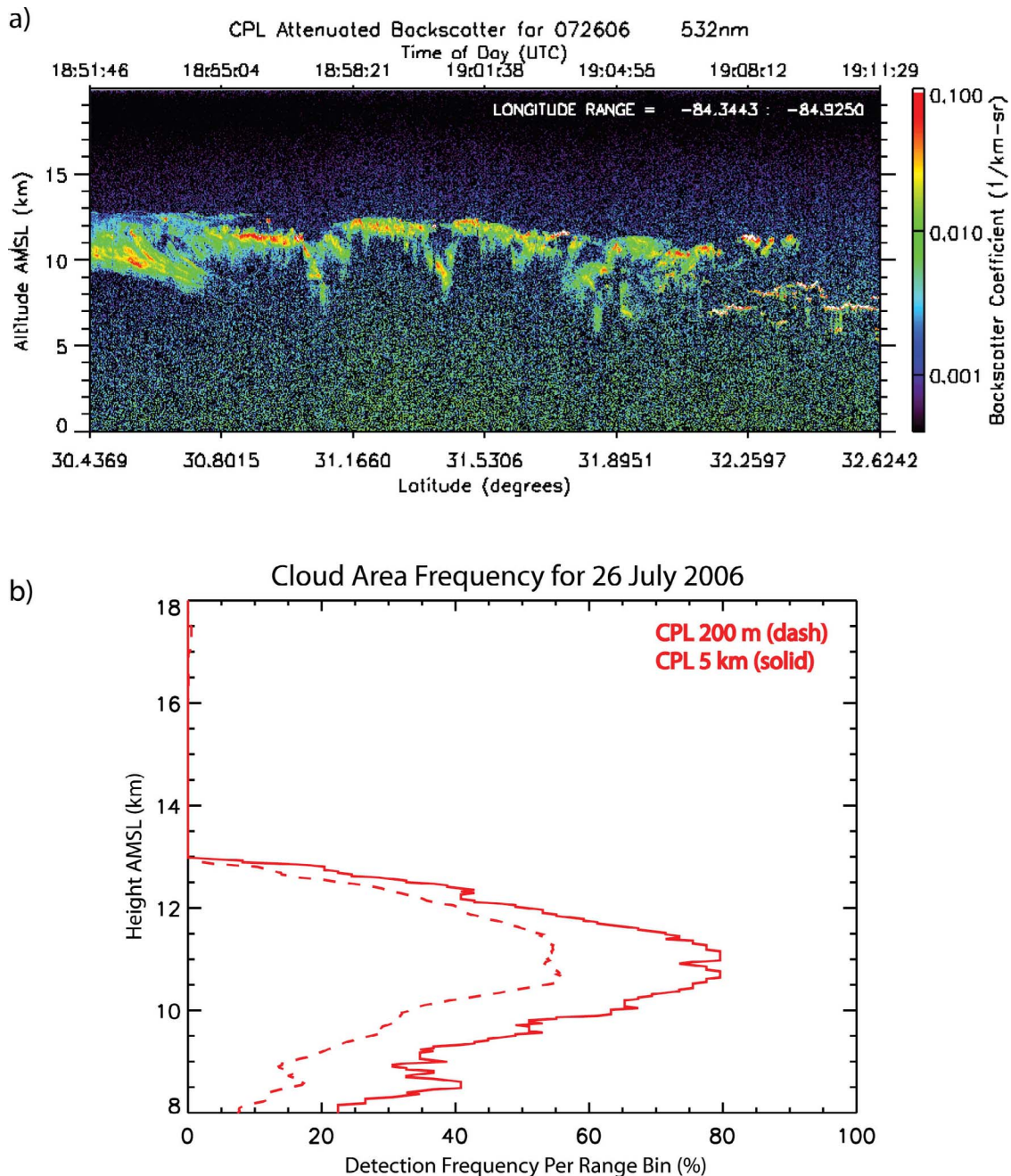
Figure 1. (a) Attenuated total backscatter (km^{-1} sr^{-1}) from the airborne CPL instrument (200 m) for 26 July 2006 during the daytime coincident segment shown in Table 2 demonstrates the inhomogeneous atmospheric segment observed. (b) Also plotted is the CPL cloud area detection frequency per range bin normalized to the total number of range bins in the same 26 July 2006 segment at spatial resolutions of 200 m (dashed) and 5 km (solid).

compare the two instruments on identical SNR scales [*Young and Vaughan*, 2009].

[8] Multiple scattering is primarily a function of particle properties (number density, size distribution, and shape) and sensing geometry of the lidar (FOV and distance to the scattering media) [*Eloranta*, 1998]. Multiple scattered photons scattered within the forward diffraction peak of the phase function will travel along with the main laser pulse and contribute to the lidar backscatter. This contribution can be significant both within the cloud and in the molecular atmosphere below the cloud. The multiple scattering effectively reduces the optical depth of the scattering layer. Even though CALIOP and CPL have similar receiver FOVs, the extreme distance of CALIOP from the scattering media (~700 km) translates into a receiver footprint of nearly 90 m which allows for a more significant multiple scattering contribution to CALIOP measurements compared to CPL. Spatial properties, such the layer top and base, and retrieved of optical

Table 2. Collocation Details of CPL and CALIOP Measurements

Date (2006)	Latitude Range	Overpass (UTC)	Offset (m)
26 July	30.4 to 32.6 N	19:01:31	1317
31 July	17.2 to 19.4 N	19:16:31	557
2 Aug.	31.0 to 33.1 N	19:07:59	1252
3 Aug.	23.9 to 26.0 N	19:49:19	1317
8 Aug.	35.5 to 33.3 N	7:29:50	61
10 Aug.	33.7 to 31.6 N	7:18:00	170
11 Aug.	38.2 to 36.2 N	8:00:00	498
12 Aug.	33.2 to 31.0 N	7:05:50	37
13 Aug.	28.6 to 30.8 N	18:49:00	1716
14 Aug.	36.4 to 38.5 N	19:34:26	1430

properties like extinction and optical depth are influenced by the multiple scattering effects differently. The spatial properties are only influenced by multiple scattering in cases where the atmospheric layer is totally attenuating. CALIOP having more significant multiple scattering effects will be able to penetrate much further into an opaque layer than CPL. Multiple scattering effects on the layer optical properties are parameterized using a multiple scattering correction factor (η) that is applied to either the extinction coefficient [*Platt*, 1981] or in the case of CALIOP, the optical depth term [*Winker*, 2003] of the single scattering lidar equation. The η term accounts for the apparent increase in two-way transmittance that occurs as a result of multiple scattering. For lidar instruments where there is no multiple scattering, $\eta = 1$. For CPL measurements of thin cirrus, only 5% or less of the total backscattered signal can be attributed to multiple scattering, and multiple scattering effects are no more than 15% for cloud layers with an optical depth of 2.0 [*McGill et al.*, 2002]. Thus η is estimated to be no greater than 0.96 for CPL cirrus cloud measurements. In contrast, CALIOP uses a constant value of $\eta = 0.6$ for all cirrus clouds that is assumed to be independent of range and optical depth [*Young and Vaughan*, 2009]. For CALIOP cirrus layer detection presented in this study, the extra pulse penetration phenomena of opaque layers is most important and will be explored in section 5.

3. Coincident Measurements

[9] During the period of 26 July to 14 August 2006, ER-2 aircraft flights were conducted out of Warner-Robbins, GA as part of the CALIPSO-CloudSat Validation Experiment (CC-VEX) [*McCubbin et al.*, 2006]. These flights were planned over land and ocean surfaces, targeting subtropical cirrus and convective anvils with a scientific objective of simultaneously validating multiple measurements made by the NASA A-Train of satellites, especially CALIPSO and CloudSat [*Stephens et al.*, 2002]. CPL was a payload on a total of 12 ER-2 flights which included ten coincident segments and four flights during nighttime hours to permit analysis of night versus day performance [*McGill et al.*, 2007].

[10] The validation procedure implemented during CC-VEX directed the ER-2 aircraft to fly the predicted ground track of the CALIPSO satellite for 30 to 40 min centered on the predicted overpass time, creating a coincident segment of up to 4 degrees latitude in length. However, the collocation was imperfect because the predicted ground track was not exact. Table 2 provides information on the latitude ranges of each segment, as well as exact coincident times and

ground track offsets. The ground track offset at the exact coincident time between the satellite and the aircraft during the ten analyzed flights averaged 835 m, but ranged from 37 to 1716 m. Since the CPL footprint is small compared to CALIPSO, the two instruments do not observe exactly the same cloud scene. Therefore, the assumption that the cloud scene is horizontally homogeneous must be invoked in this study. Another main complication of the validation of satellites from aircraft is the large difference in relative speed. The 4 degrees of latitude are sampled by CALIPSO in approximately 70 s (~7500 m/s) compared to 40 min with the ER-2 (~200 m/s). This time discrepancy increases uncertainties in the assumption of horizontal homogeneity in the coincident segment, particularly at distances further away from the exact coincident point. For this study, we restrict the analysis to within ±10 min CPL time of the exact coincident point, resulting in a segment approximately 2 degrees latitude in length (20 min CPL time) centered at the exact coincident second for each of the ten flights with coincident CALIPSO data (Table 2). Assuming a validation target of cirrus layers, a segment of this extent provides enough data points for meaningful statistical analysis, yet minimizes the uncertainties in the horizontal homogeneity assumption.

4. CPL and CALIPSO Layer Detection Algorithms

[11] Particulate layers, such as aerosol and cloud layers, increase the CPL and CALIOP backscatter signal relative to the expected molecular backscatter, thus making them distinguishable from the clear-air troposphere [*McGill et al.*, 2007; *Vaughan et al.*, 2009]. Data processing algorithms then resolve the physical and optical properties of these cloud and aerosol layers. The routine CALIOP data processing generates both level 1 and level 2 data. The level 1 data includes geolocated and calibrated backscatter data [*King et al.*, 2004]. The level 2 products, which are the focus of this paper, report physical and optical properties of both clouds and aerosols [*Vaughan et al.*, 2004]. *Winker et al.* [2009] describe the overall CALIOP science data processing architecture. There are three primary processing algorithms used to derive physical and optical properties in the level 2 data: layer detection, scene classification, and extinction retrieval. *Young and Vaughan* [2009] explains the hybrid extinction retrieval algorithm (HERA). The scene classification algorithm (SCA) contains submodules to discriminate between clouds and aerosol layers [*Liu et al.*, 2004, 2009], classify aerosol layers [*Omar et al.*, 2005, 2009] and distinguish liquid water and ice phase clouds [*Hu et al.*, 2009].

[12] The CALIOP selective, iterated boundary locator (SIBYL) detects cloud and aerosol layers in the CALIOP backscatter signals [*Vaughan et al.*, 2009]. A generic profile scanning engine is embedded in the SIBYL algorithm. This profile scanning engine is repeatedly invoked by an iterated, multiresolution spatial averaging scheme, which averages data to increasing coarse resolutions up to 80 km horizontal data segments. Use of this procedure overcomes the CALIOP SNR limitations previously described and enables more accurate detection of optically thin features [*Vaughan et al.*, 2009]. The expected molecular backscatter signal and magnitude of the background noise in the profile being examined

are then used to build a range-varying detection threshold for each invocation of the profile scanning engine. During the profile scanning process, the threshold values are revised as necessary to account for the attenuation of any atmospheric layers encountered [*Vaughan et al.*, 2005]. Due to the space-based nature of the CALIOP instrument, the SIBYL has been designed for automated detection of the vertical and horizontal extent of cloud and aerosol layers, irrespective of the varying layer types that may be present in the lidar profile. The SCA module handles the subsequent task of distinguishing one layer type from another (e.g., clouds from aerosols). More detailed information on the complete SIBYL algorithms is presented by *Vaughan et al.* [2009], with prelaunch implementation described by *Vaughan et al.* [2005].

[13] At cirrus cloud altitudes, CALIOP version 3, level 2 cloud layer products are reported at horizontal spatial resolutions of 1 and 5 km. CPL attenuated backscatter signals are therefore averaged to 1 and 5 km horizontally for this study. This averaging is achieved with geo-location matched to CALIPSO so that each CPL and CALIOP profile is averaged over an identical latitude range (to within 0.01 degrees). Unlike the CALIOP SIBYL algorithms, the CPL layer detection algorithm processes data at a single spatial resolution to detect layers [*McGill et al.*, 2003]. For this study, cloud layers are detected at 1 and 5 km spatial resolutions using the standard CPL processing algorithms, which proceed as follows. The mean attenuated total backscatter coefficient for vertical segments of 1 km is determined for each profile. If this mean value is less than the attenuated molecular backscatter coefficient of a modeled standard clear-atmosphere, then the value is unchanged. If the mean attenuated total backscatter coefficient is greater than the modeled attenuated molecular backscatter coefficient due to the presence of a particulate layer, the modeled attenuated molecular backscatter coefficient is used as the mean of the 1 km segment. A profile is constructed by interpolating a value for each bin between segment mean bins. A threshold profile is computed as the sum of the interpolated profile and a constant multiple (modeled using CPL data) of the square root of the variance of the raw signal in the background region [*Palm et al.*, 2002] that has been normalized by the range squared for each bin and the energy of the lidar shot. The constant multiplier is adjusted for spatial resolution and geographic location for each flight, but remains the same for all layer types. Similar to SIBYL, the threshold is corrected for attenuating layers present in the profile data. Starting from the top of the profile, a layer is identified when the attenuated backscatter coefficient is above this threshold for three consecutive range bins. The top height of the layer is located at the height where the highest of the consecutive samples is found. The base height of the layer is the bin just above where the first of three consecutive particle-free regions (i.e., where the attenuated backscatter coefficient is less than this threshold) is determined [*Palm et al.*, 2002].

5. Assessment of CALIPSO Cirrus Cloud Layer Detection

[14] An examination of the CALIPSO cirrus cloud layer detection is performed for both the 1 and 5 km level-2 version-3 standard cloud layer products using CPL data at identical spatial scales. While the CALIPSO 1 km cloud layer product only reports layers detected at horizontal resolutions of 1 km, the CALIPSO 5 km cloud layer product reports layers detected at horizontal resolutions of 5, 20 and 80 km. As previously noted, implementation of this multiresolution averaging scheme was deemed necessary to overcome the SNR limitations of the CALIOP instrument [*Vaughan et al.*, 2009]. Therefore, to compare the two instruments on identical spatial scales, the 'horizontal averaging' field in the CALIOP layer products must be queried to identify those cloud layers detected at 5 km only. However, since the standard 5 km layer product reports cloud layers detected at resolutions as high as 80 km, the two instruments can also be compared on a more similar SNR scale but with the caveats of spatially averaging numerous profiles as described in section 2 (Figure 1). To minimize the false horizontal broadening of cloud layers due to averaging the signal, the CALIPSO algorithm applies a minimum integrated attenuated backscatter threshold to all candidate layers [*Vaughan et al.*, 2009]. To make effective use of the 5 km cloud layer product, users should be aware of this trade-off between SNR and spatial resolution.

[15] The validation includes a direct comparison of cloud layer boundaries for all ten coincident flights. In this study we present two CC-VEX cases; 31 July 2006 during local daytime and 11 August 2006 at local nighttime. The cloud top and base altitudes from the CALIOP cloud layer product and CPL averaged product are used to create cloud mask profiles of in-cloud (1) or out-of-cloud (0) bins for each averaged lidar profile at the 30 m vertical bin resolution of CPL. These cloud locations are then compared for the 2 degree latitude coincident segment length, centered on the point of coincidence, for each CALIPSO overpass. The CPL and CALIOP cloud mask profiles are co-aligned both horizontally and vertically. Finally, statistics of cloud detection are developed from bin-to-bin comparisons of the cloud mask profiles. The standard 200 m CPL layer detection product, with high SNR and high resolution, will be considered the "true cloud scene" for transparent cirrus layers.

5.1. Case Studies

[16] The 31 July case shown in Figure 2 is a good representation of a daytime segment in which both optically thick and optically thin cirrus clouds are present. The segment analyzed was obtained just east of the Yucatan Peninsula, between 17.20 N and 19.36 N degrees latitude, during local daytime hours. The direct overpass was at 19:16:31 UTC, at which time the ER-2 was 557 m off the satellite ground track. Figure 2 shows the full resolution attenuated total backscatter ($km^{-1}\ sr^{-1}$) from both 200 m CPL data (Figure 2a, with the CPL 200 m cloud boundaries in red) and 333 m CALIOP data (Figure 2b) for the segment. There are numerous optically thick cirrus clouds between 8 and 14 km, specifically between 18.00 N and 18.65 N and again from about 18.50 N to 19.36 N, that are discernible in the attenuated backscatter images of both instruments. The CPL and CALIOP cloud layer boundaries are plotted for the segment at a horizontal resolution of 5 km in Figure 3a. The 5 km CALIOP cloud boundaries (blue) are in good agreement with 5 km CPL cloud boundaries (red) for the two optically thick cirrus clouds between 10 and 14 km. Similarly, when considering all clouds present in the scene, the combined CALIOP results from the 5-20-80 km resolutions
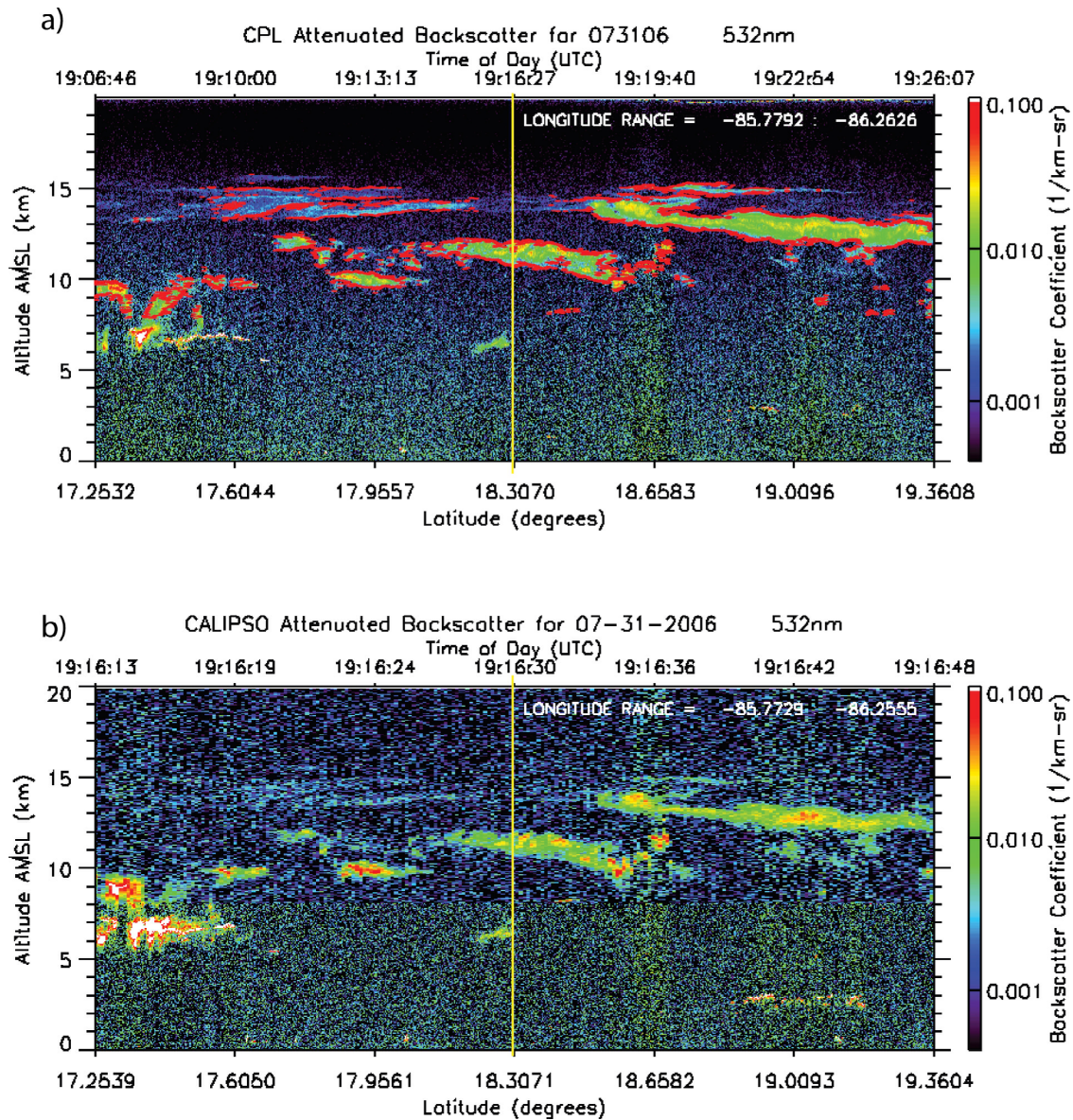
Figure 2. Attenuated total backscatter (km^{-1} sr^{-1}) from (a) the airborne CPL instrument and (b) the CALIOP instrument onboard CALIPSO for 31 July 2006 during a daytime coincident overpass located east of Belize in the Caribbean Sea. Both images are shown at the native resolution. The red outline in the CPL figure displays the 200 m cloud boundaries and the yellow line represents the exact point of coincidence.

are in good qualitative agreement with the CPL results (Figure 3b).

[17] To quantify the degree of agreement between the two sets of results we used the following procedure. For each 30 m height bin, the total number of bins detecting a cloud in a given segment was divided by the total number of observed bins to provide vertical profiles of cloud area frequencies, shown for this segment in Figure 4 for spatial resolutions of 5-20-80 km (Figure 4a) and 1 km (Figure 4b). There is very good agreement between CPL (solid red) and CALIOP (solid blue) for both 1 and 5 km resolutions below 11 km, where optically thick cirrus clouds are prevalent in the segment. The 5 km products of both instruments yield higher cloud area frequencies in this altitude region than the 200 m

CPL product, as expected due to the caveats of averaging the data discussed previously.

[18] There are also optically thin cirrus clouds observed in this 31 July segment (13–15 km) between 17.26 N and 18.31 N that are easily distinguishable in the CPL measurement, but appear faint in the CALIPSO attenuated backscatter image (Figure 2). CPL detects the optically thin cirrus cloud boundaries between 13 and 15 km at a resolution of 5 km, as illustrated in Figure 3. However, the CALIOP layer detection algorithm fails to detect the optically thin cirrus cloud boundaries between 17.26 N and 18.31 N at a resolution of 5 km (Figure 3a). Furthermore, the CALIOP cloud area frequencies at 5 km (solid blue) are 20–50% lower than the CPL 5 km cloud area frequencies (solid red) plotted in
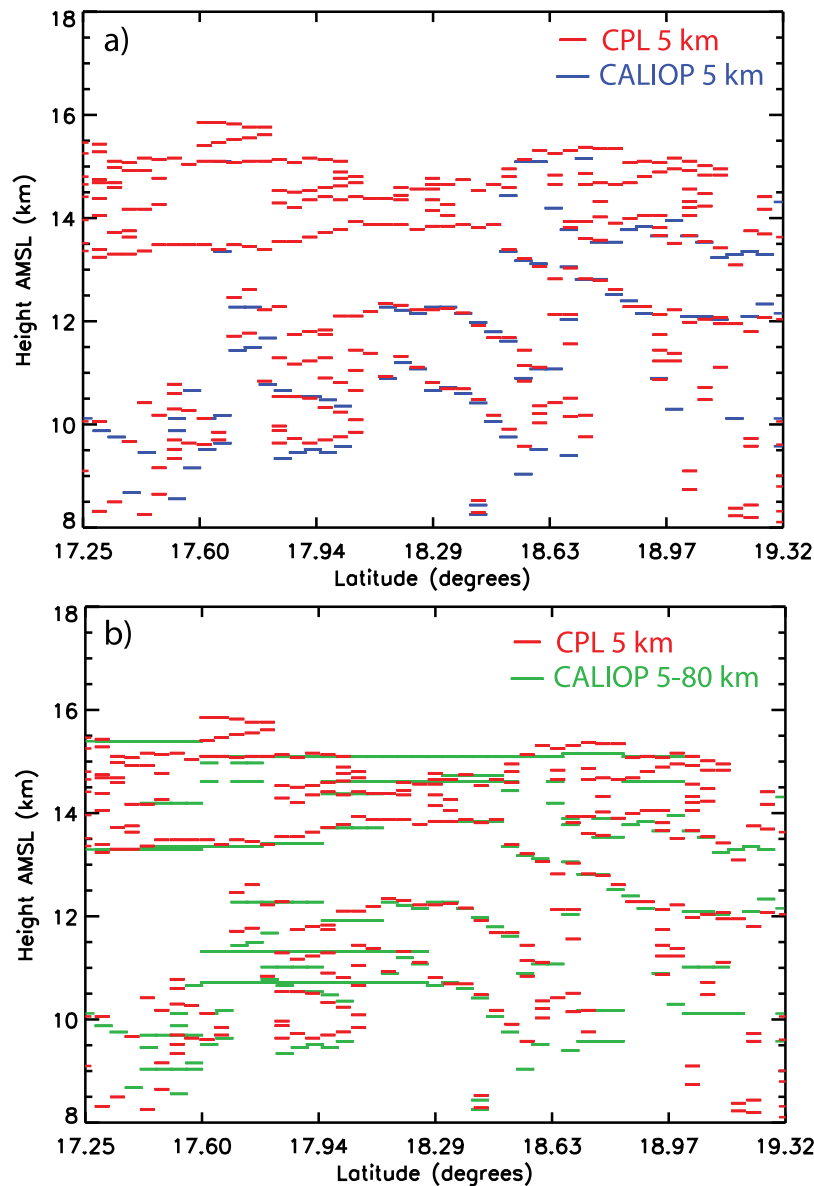
Figure 3. Cloud boundaries retrieved from CPL and CALIOP for 31 July 2006 during the daytime coincident segment in Figure 2. The CPL 5 km cloud boundaries (red) are shown in both plots, with (a) the CALIOP 5 km horizontally averaged cloud boundaries displayed in blue and (b) the CALIOP 5-20-80 km cloud boundaries displayed in green.

Figure 4a for altitudes greater than 13.0 km. A similar result is found at a spatial resolution of 1 km (Figure 4b). This disagreement between the two instruments at identical spatial scales is a consequence of the lower CALIOP SNR during daytime hours. When the CALIOP SNR is increased by using resolutions of 5-20-80 km to detect cloud layers (Figure 3b), the CALIOP layer boundaries (green) are in much better agreement with the CPL 5 km cloud boundaries (red). Additionally, CALIOP 5-20-80 km cloud area frequencies (dashed blue) are in much better agreement with CPL 5 km cloud area frequencies (solid red) above 13 km (Figure 4a). However, averaging the signal is inaccurately identifying broken cirrus clouds as one horizontally homogeneous layer. An example of this phenomenon is illus-

trated in Figure 3b (green) between 17.60 and 18.29 N and 10.5 and 12.0 km where CPL does not detect a cloud at 5 km. This phenomenon causes the CALIOP 5-20-80 km cloud area frequency (Figure 4, dashed blue) between 10.5 and 12.0 km to be 20–30% higher than the CPL and CALIOP 5 km cloud area frequencies. Uncertainties in the assumption that the instruments are observing the same cloud scene can also cause disagreement between the two instruments. CPL and CALIOP are likely detecting different cloud scenes in Figures 2 and 3 between 17.25 and 17.60 N.

[19] The segment analyzed on 11 August exemplifies good cloud area agreement between CPL and CALIPSO during nighttime for both opaque and transparent optically thick clouds above the CPL cloud base. This segment was acquired
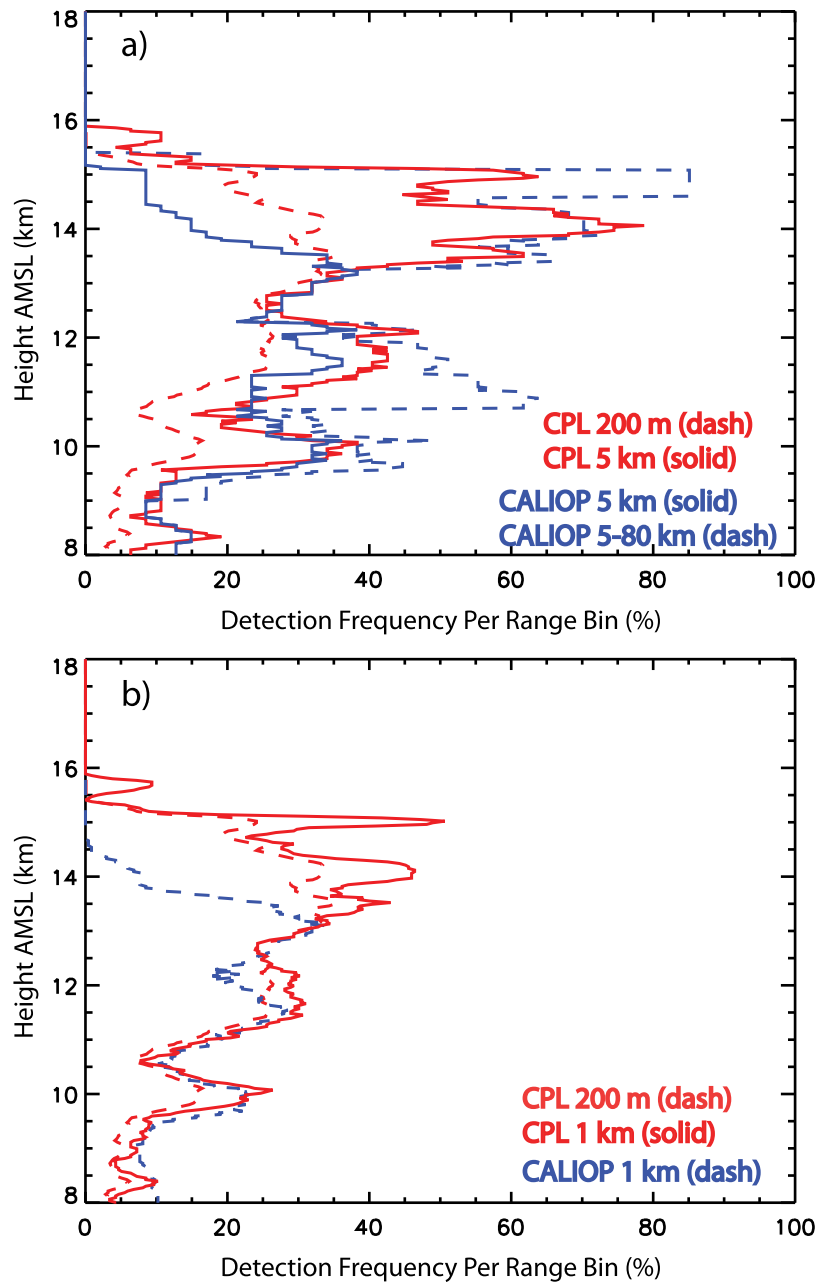
Figure 4. Cloud area detection frequency per range bin normalized to the total number of range bins in the daytime coincident segment of 31 July 2006. (a) The CPL 200 m (dashed red) and 5 km (solid red) frequencies are compared to the 5 km (solid blue) and 5-20-80 km (dashed blue) CALIOP frequencies. (b) Also, the CPL 200 m (dashed red) and 1 km (red) frequencies are compared to the 1 km CALIOP frequencies.
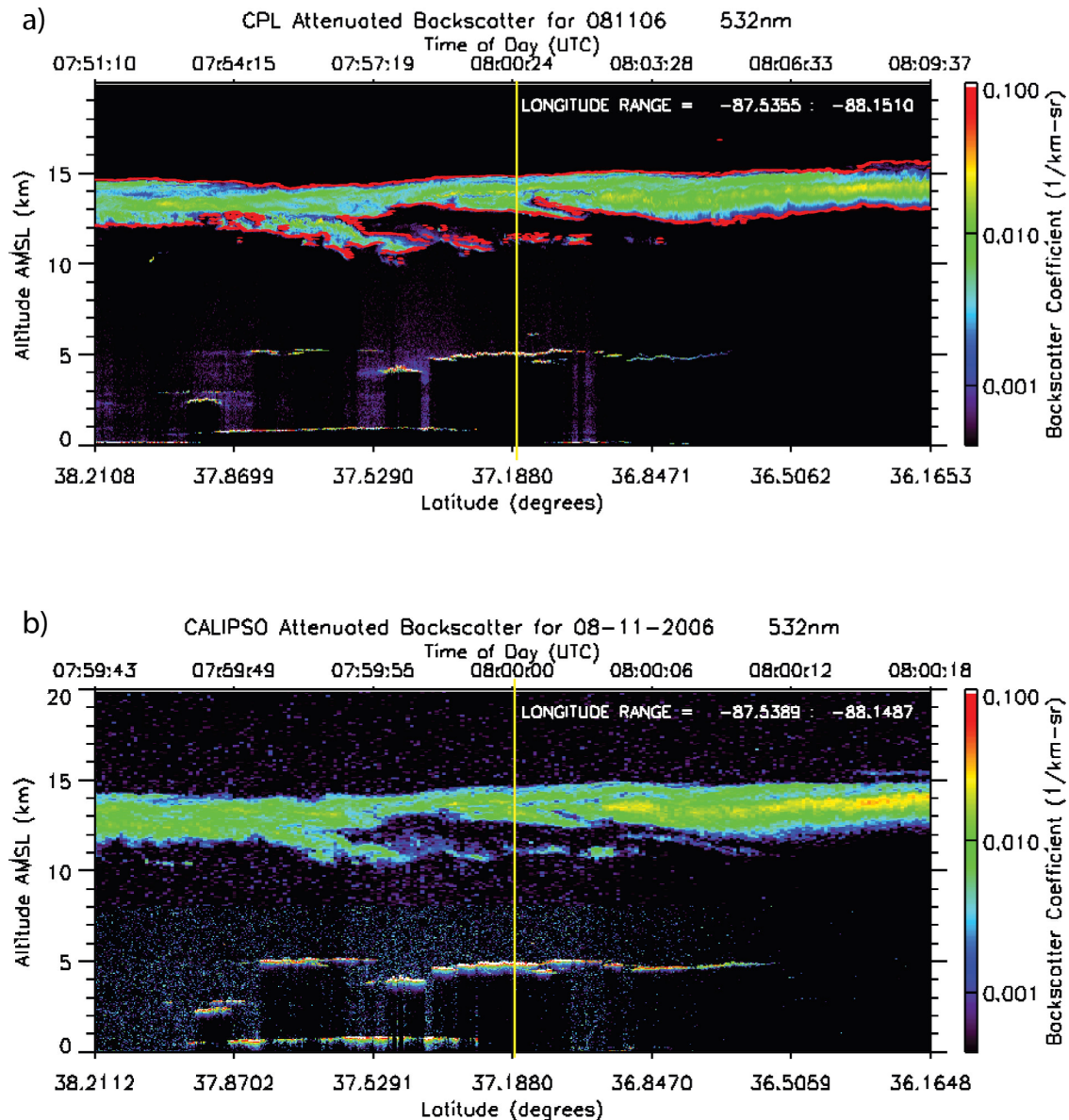
Figure 5. Attenuated total backscatter (km^{-1} sr^{-1}) from (a) the airborne CPL instrument and (b) the CALIOP instrument onboard CALIPSO for 11 Aug. 2006 during a daytime coincident overpass located in the southeastern United States. Both images are shown at the native resolution. The red outline in the CPL figure displays the 200 m cloud boundaries.

over the southeastern United States between 36.16 N and 38.21 N degrees latitude, during local nighttime hours. The exact coincident time was at 08:00:00 UTC, at which time the ER-2 was 498 m off the satellite ground track. As observed in the attenuated backscatter for the segment (Figure 5) from both CPL (Figure 5a) and CALIPSO (Figure 5b), the SNR is greater during this nighttime overpass than the 31 July case, and therefore more consistent detection of cloud area by both instruments is observed. There is one optically thick cirrus cloud which stretches throughout the entire segment between 12 and 15 km, discernible in the attenuated backscatter images from both instruments. The cloud layer boundaries are plotted for the segment in Figure 6. The 5 km CALIOP cloud top boundaries (blue) are in excellent agreement with 5 km CPL cloud top

boundaries (red) for this optically thick cirrus cloud. The RMS difference for the cloud top boundaries is 216 m. Furthermore, Figure 7 shows CPL (solid red) and CALIOP (solid blue) cloud area frequencies for both 1 (Figure 7b) and 5 km (Figure 7a) resolutions that are nearly identical above 14 km. These cloud area frequencies above 14 km are also in excellent agreement with the 200 m CPL results for the same altitude range.

[20] While the cloud top altitudes agree well, there is considerable disagreement between the two instruments on the location of the cloud base for the cirrus clouds measured on 11 August 2006. The RMS difference for the cloud base boundaries is 1540 m. CPL detects cloud base boundaries that are consistently 0.5 to 2.0 km higher than both the CALIOP 5 km and 5-20-80 km data (Figure 6). Additionally,
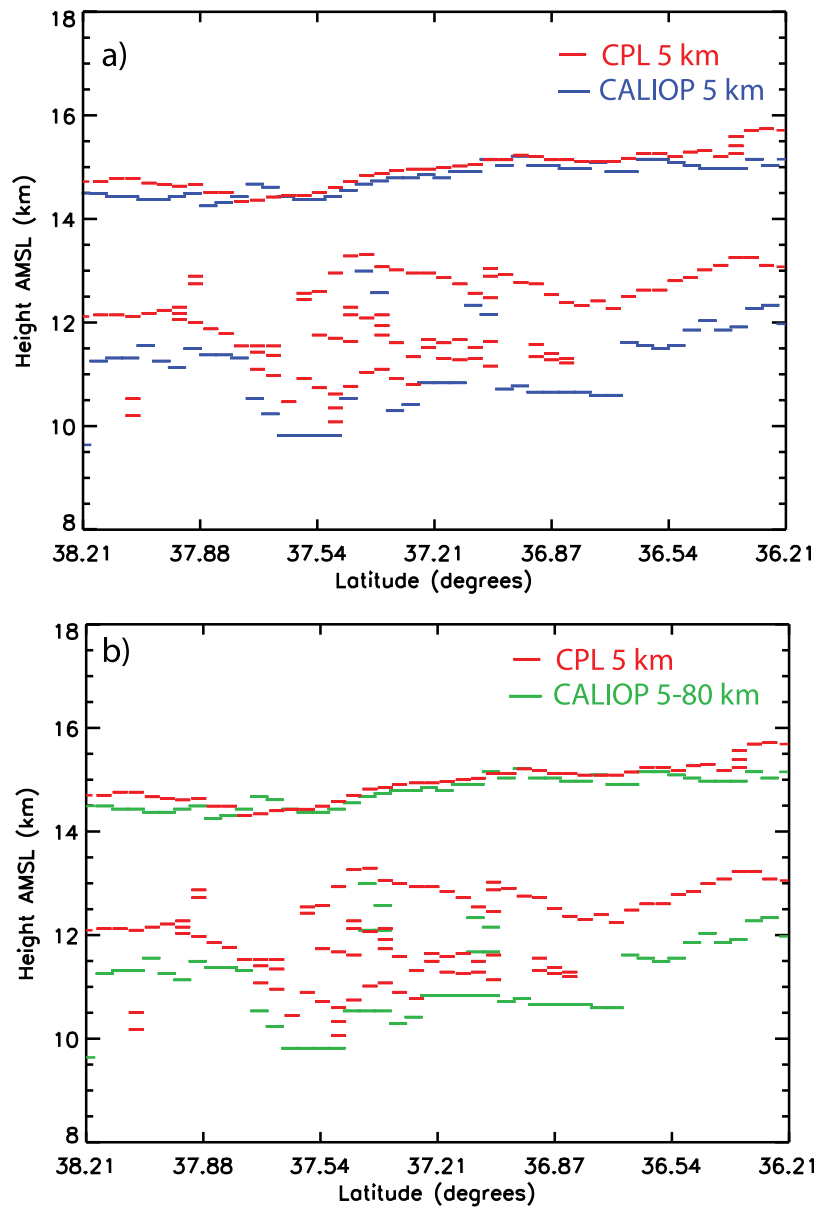
Figure 6. Cloud boundaries retrieved from CPL and CALIOP for 11 Aug. 2006 during the daytime coincident segment in Figure 5. The CPL 5 km cloud boundaries (red) are shown in both plots, with (a) the CALIOP 5 km horizontally averaged cloud boundaries displayed in blue and (b) the CALIOP 5-20-80 km cloud boundaries displayed in green.

CPL cloud area frequencies are 10–60% lower than CALIOP cloud area frequencies at altitudes less than 13 km and a horizontal resolution of 5 km (Figure 7). These higher cloud area frequencies derived by CALIOP are observed in both opaque and transparent layers. We define a CPL opaque layer as any layer in which no enhanced backscatter signal was observed below the layer as a consequence of another layer or the Earth's surface. All other CPL layers are defined as transparent. CALIOP uses a similar technique to determine opaque layers: within any 5-km averaged profile, the lowest layer detected is defined as opaque if the Earth's surface is not detected. These layers are identified by the CALIOP opacity flag provided in the standard data product.

[21] Cloud layers observed in profiles between 36.51 N and 36.16 N in the attenuated backscatter images of both instruments (Figure 5) are considered to be opaque since no ground signal or lower particulate layer is detected. The CALIOP cloud area frequencies at resolutions of 5 km and 5-20-80 km are higher than the CPL 5 km cloud area frequencies between 11.5 and 12.5 km for opaque layers (Figure 8b). Additionally, Figure 9 shows 200 m CPL cloud base boundaries (red lines) that are about 1–2 km higher than the bottom of the cirrus layer inferred by the CALIOP 1 km attenuated total backscatter (km^{-1} sr^{-1}) between 36.51 N and 36.16 degrees latitude. This disparity in cloud base boundaries between the two instruments is attributed to
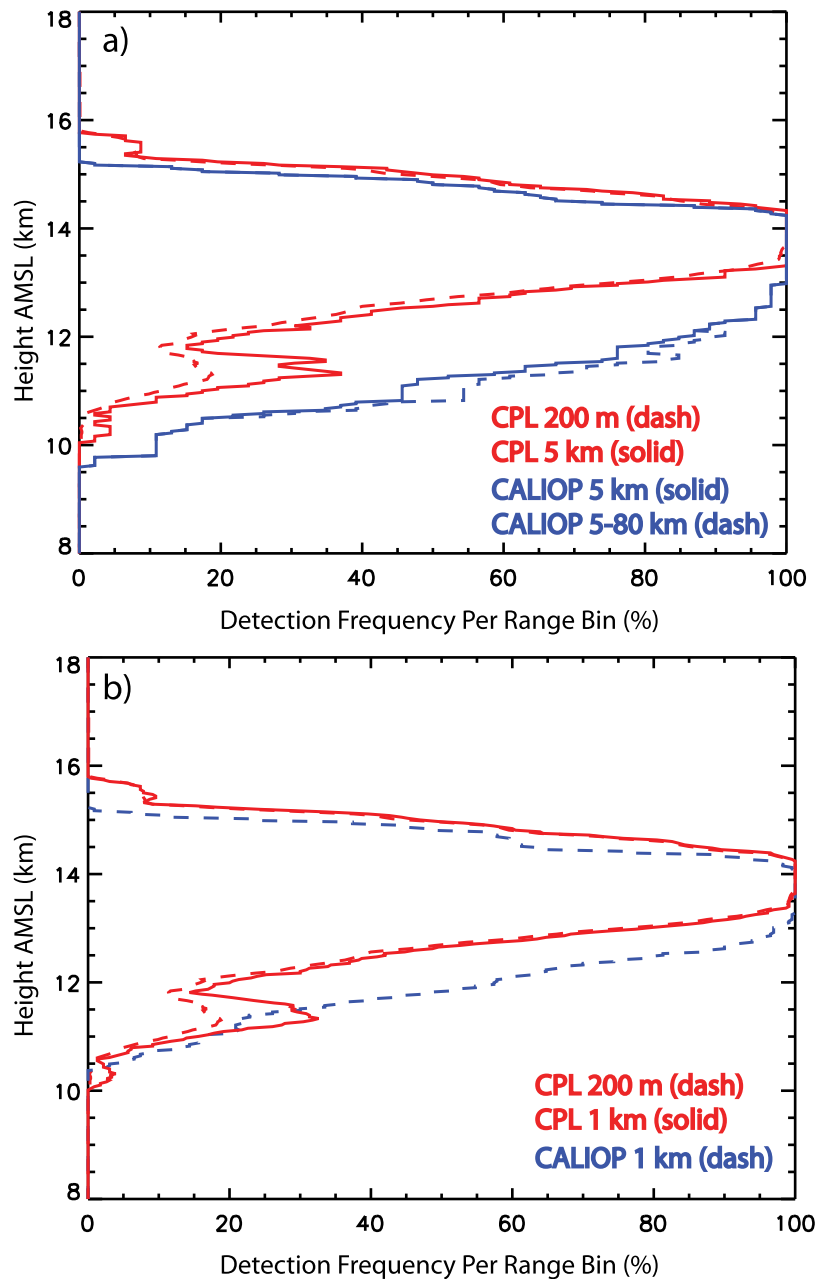
Figure 7. Cloud area detection frequency per range bin for the daytime coincident segment of 11 Aug. 2006 at CALIOP horizontal resolutions of (a) 5 and 5-20-80 km and (b) 1 km.

multiple scattering. Although the CALIOP cirrus transmittance and optical depth retrievals are corrected for multiple scattering effects, these effects can greatly enhance CALIOP penetration into ice clouds compared to CPL, since the transmittance of a light beam through a cloud is increased [*Young and Vaughan*, 2009]. This phenomenon is noticeable in the CALIOP signal only when completely opaque clouds such as the clouds sampled in this 11 August segment are observed.

[22] Cirrus cloud layers observed in profiles from 38.21 N to 36.51 N in the attenuated backscatter images of both instruments (Figure 5) are considered to be transparent since a ground signal or lower cloud layer is detected. Therefore,

the CPL data should be a good representation of the true cloud scene. The CALIOP cloud area frequencies at resolutions of 5 km and 5-20-80 km are 10–50% higher (below 13 km) than the CPL 5 km cloud area frequencies for transparent layers (Figure 8a). The CALIOP "Closing gap between features" technique [*Vaughan et al.*, 2005] completely closes the vertical distances between the physically small broken clouds (11 km) observed in Figure 5 between 37.54 and 36.87 N and the large optically thick cloud (13–15 km), making it one cloud of larger vertical extent. For the CALIOP version 3 data products, vertically adjacent layers detected in a single profile that are separated by 0.48 km or less are merged into single layers. The CPL algorithms
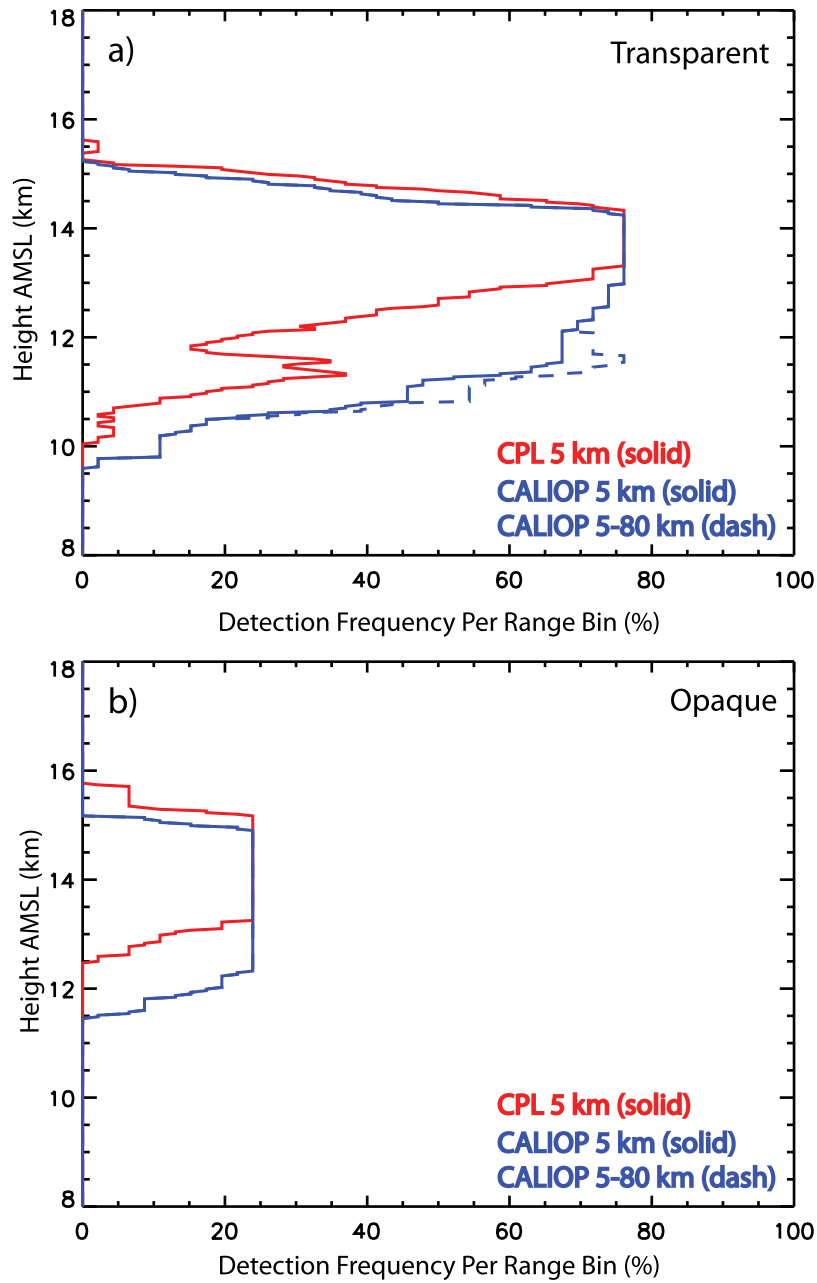
Figure 8. Cloud area detection frequency per range bin for the nighttime coincident segment of 11 Aug. 2006 is plotted with altitude for (a) transparent and (b) opaque layers at horizontal resolutions of 5 km.
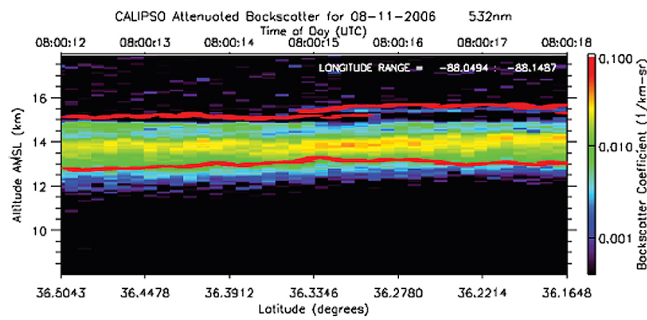
Figure 9. Attenuated total backscatter (km^{-1} sr^{-1}) from the CALIOP instrument (1 km resolution) between 36.50 N and 36.16 N for 11 Aug. 2006 in which the cirrus layer shown is considered opaque. The red lines display the 200 m cloud boundaries as determined by CPL.

do not combine the two cloud layers, thus it detects two separate cloud layers, resulting in the secondary maximum in CPL 5 km cloud area frequency between 11.0 and 11.5 km observed in Figure 7 and Figure 8a. Cloud layers reported in the CPL data can be separated by as little as 90 m.

5.2. CC-VEX Statistics

[23] Composite statistics are computed for all cloud layers above 8 km. Separate sets of statistics are also computed for daytime, nighttime, opaque and transparent cloud layers observed during the ten CALIPSO overpasses from the CC-VEX campaign (Tables 3, 4 and 5). At a horizontal resolution of 5 km, CPL and CALIOP detect clouds in 16.2% and 17.3%, respectively, of 158,841 total range bins (clear and cloudy, Table 3). The associated 5-20-80 km cloud area frequencies for all collocated data are plotted in the upper panels of Figure 10 for daytime conditions (Figure 10a) and nighttime conditions (Figure 10b) for all cloud opacities. Figure 10 shows cloud area frequencies for all opaque cloud layers (Figure 10c) and all transparent cloud layers (Figure 10d) for cloud layers detected at all hours of the day. Similar plots for the 1 km cloud area

frequencies are shown in Figure 11. Cloud area frequencies for daytime conditions (Figure 10a) are very similar to those observed in the 31 July case. For cloud layers below 11 km, there is good agreement between the 5 km cloud area frequencies of the two instruments. However, CALIOP 5 km cloud area frequencies (solid blue) above 13 km are 5–20% lower than CPL 5 km cloud area frequencies (solid red). Furthermore, CPL detects a cloud where CALIOP does not detect a cloud in 6.1% of total daytime bins at a horizontal resolution of 5 km (Table 3). The majority of these 6.1% of bins are most likely a consequence of the lower CALIOP SNR discussed in section 2. Similar results are found for cloud area frequencies at 1 km spatial resolutions (Figure 11a and Table 4). If the CPL 5 km cloud area frequencies are compared to the 5-20-80 km CALIOP cloud area frequencies, to evaluate the two instruments on a more similar SNR scale, much better agreement is observed (Figure 10). The percentage of bins in which CPL detects a cloud but CALIOP does not reduces to 3.9% (Table 5). This remaining 3.9% of bins can still be attributed to lower CALIOP SNR and uncertainties in the assumption that the instruments are observing the same cloud scene as demonstrated in the 31 July case.

[24] Cloud area frequencies for nighttime conditions (Figure 10b) are very similar to those observed in the 11 August case. For cloud layers above 14 km, there is excellent agreement between the 5 km cloud area frequencies of the two instruments. The two instruments can be compared for cloudy bins determined by CPL using Table 3 and dividing the "Both In" category by the sum of the "Both In" and "CPL in, CALIOP out" categories. When CPL detects a cloudy bin, CALIOP also detects a cloudy bin in 88.8% of bins at a horizontal resolution of 5 km. This percentage increases to 94.1% when comparing 5-20-80 km CALIOP data to 5 km CPL data (Table 5). The percentage of total nighttime bins in which CPL detects a cloud but CALIOP (5-20-80 km) does not is only 1.3% (Table 5). This excellent agreement is a result of the higher SNR of both instruments, coupled with the horizontally homogeneous structure of the optically thick clouds observed during the four nighttime cases. However, there is disagreement between the 5 km

Table 3. Bin-By-Bin Comparison of CPL and CALIOP During CC-VEX: 5 km Data[a]

	Total	CPL In	CALIOP In	Both In Cloud	CPL In, CALIOP Out	CALIOP In, CPL Out	Both Out
				All Cloud Layers			
POINTS	158841	25762	27453	18411	7351	9042	124037
FREQ	100.0	16.2	17.3	11.6	4.6	5.7	78.1
				Daytime			
POINTS	94572	11645	9183	5880	5765	3303	79624
FREQ	100.0	12.3	9.7	6.2	6.1	3.5	84.2
				Nighttime			
POINTS	64269	14117	18270	12531	1586	5739	44413
FREQ	100.0	22.0	28.4	19.5	2.5	8.9	69.1
				Transparent Cloud Layers			
POINTS	158841	19968	18598	11577	8391	7021	131852
FREQ	100.0	12.6	11.7	7.3	5.3	4.4	83.0
				Opaque Cloud Layers			
POINTS	158841	5794	8855	4347	1447	4508	148539
FREQ	100.0	3.6	5.6	2.7	0.9	2.8	93.5

[a]Height range: 8.0 km to 18.0 km.

Table 4. Bin-By-Bin Comparison of CPL and CALIOP During CC-VEX: 1 km Data[a]

	Total	CPL In	CALIOP In	Both In Cloud	CPL In, CALIOP Out	CALIOP In, CPL Out	Both Out
				All Cloud Layers			
POINTS	794205	110192	108365	76521	33671	31844	652169
FREQ	100.0	13.9	13.6	9.6	4.2	4.0	82.1
				Daytime			
POINTS	472860	42691	34610	19624	23067	14986	415183
FREQ	100.0	9.0	7.3	4.2	4.9	3.2	87.8
				Nighttime			
POINTS	321345	67501	73755	56897	10604	16858	236986
FREQ	100.0	21.0	23.0	17.7	3.3	5.2	73.7
				Transparent Cloud Layers			
POINTS	794205	82835	65583	44997	37838	20586	690784
FREQ	100.0	10.4	8.3	5.7	4.8	2.6	87.0
				Opaque Cloud Layers			
POINTS	794205	27357	42782	20795	6562	21987	744861
FREQ	100.0	3.4	5.4	2.6	0.8	2.8	93.8

[a]Height range: 8.0 km to 18.0 km.

cloud area frequencies of the two instruments for cloud layers below 14 km during nighttime hours. Figure 10b yields CALIOP 5 km cloud area frequencies (solid blue) below 14 km that are 25% higher than CPL 5 km cloud area frequencies (solid red). Overall, CALIOP detects a cloud where CPL does not detect a cloud in 8.9% of total nighttime bins at a horizontal resolution of 5 km (Table 3). More than one-third (37.2%) of this disagreement is the result of the multiple scattering influences causing deeper penetration into opaque clouds in the CALIOP data. The remaining fraction (62.8%) is likely due to the "Closing gap between features" technique demonstrated in the 11 August case and the caveats of averaging the data to 20 and 80 km in the CALIOP detection scheme.

[25] Statistics of opaque and transparent clouds are reported in Figures 10 and 11, as well as Tables 3, 4, and 5. When CPL detects an opaque cloud, CALIOP also detects an opaque cloud in 75.0% of cloudy bins at a horizontal resolution of 5 km. CALIOP and CPL cloud area frequencies for opaque clouds are plotted in Figure 10c for 5 km and Figure 11c for 1 km. CALIOP 1 and 5 km opaque cloud area frequencies (solid blue) are consistently 5–10% higher than CPL 1 and 5 km cloud area frequencies (solid red), with the exception of cloud top boundaries. These differences are related to the multiple scattering effects in CALIOP data, which allows the CALIOP lidar to penetrate further into opaque cloud layers, similar to those found in the 11 August case. This further penetration into opaque clouds by CALIOP is actually an advantage over CPL layer detection (although it introduces uncertainty to the retrievals of optical properties) and accounts for 2.8% of total bins observed during CC-VEX collocated measurements, but is not representative of the true atmospheric scene. As demonstrated by coincident CloudSat and/or Cloud Radar System (CRS) [*Li et al.*, 2004] data, both lidar instruments are fully attenuated before the actual cloud base and therefore do not probe the full depth of the cloud [*Mace et al.*, 2009]. Thus CPL data should not be used as "truth" in opaque cloud retrievals.

Table 5. Bin-By-Bin Comparison of CPL and CALIOP During CC-VEX: 5-20-80 km Data[a]

	Total	CPL In	CALIOP In	Both In Cloud	CPL In, CALIOP Out	CALIOP In, CPL Out	Both Out
				All Cloud Layers			
POINTS	158841	25762	33666	21236	4526	12430	120649
FREQ	100.0	16.2	21.2	13.4	2.8	7.8	76.0
				Daytime			
POINTS	94572	11645	12976	7952	3693	5024	77903
FREQ	100.0	12.3	13.7	8.4	3.9	5.3	82.4
				Nighttime			
POINTS	64269	14117	20690	13284	833	7406	42746
FREQ	100.0	22.0	32.2	20.7	1.3	11.5	66.5
				Transparent Cloud Layers			
POINTS	158841	19968	24826	14358	5610	10468	128405
FREQ	100.0	12.6	15.6	9.0	3.5	6.6	80.8
				Opaque Cloud Layers			
POINTS	158841	5794	8855	4347	1447	4508	148539
FREQ	100.0	3.6	5.6	2.7	0.9	2.8	93.5

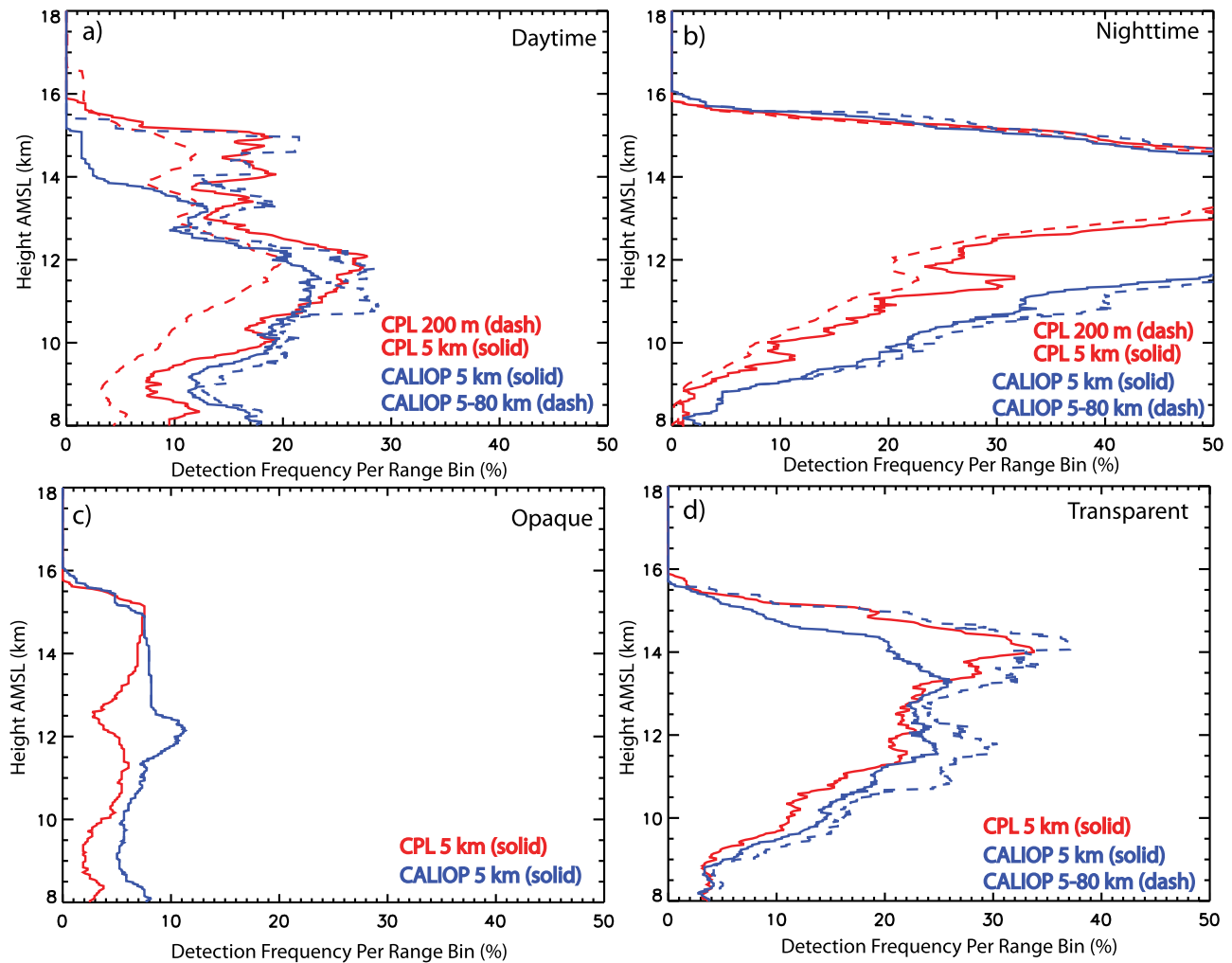[a]Height range: 8.0 km to 18.0 km.

Figure 10. Cloud area detection frequency per range bin from CPL and CALIOP for all coincident over-passes during the CC-VEX project are plotted with altitude for (a) daytime, (b) nighttime, (c) opaque cloud layers, and (d) transparent cloud layers for horizontal resolutions of 200 m, 5 km, and 5-20-80 km.

[26] Statistics of transparent clouds demonstrate occasional disagreement between the two instruments due to SNR differences, CALIOP's gap closing algorithm, and to artifacts introduced into CALIOP coarse resolution results (i.e., at 20-km and 80-km) by overestimates of the two-way transmittance of layers detected at 5-km [*Vaughan et al.*, 2005, 2009]. CALIOP and CPL cloud area frequencies for transparent clouds are plotted in Figure 10d for 5 km and Figure 11d for 1 km. CALIOP 5 km cloud area frequencies (solid blue) are 1–5% higher than CPL 1 and 5 km cloud area frequencies (solid red) for clouds below 13 km. For transparent clouds in this study, CALIOP detects a cloud when CPL does not detect a cloud in 4.4% of total bins. Some fraction of this disagreement can be contributed to CALIOP's gap closing algorithm demonstrated in the 11 August case. For high (above 13 km) optically thin clouds, CALIOP 1 and 5 km cloud area frequencies (solid blue) are 5–10% lower than CPL 1 and 5 km cloud area frequencies (solid red). This is attributed to lower CALIOP SNR and inhibits CALIOP detection of transparent clouds in 5.3% of total bins. Conversely, CALIOP 5-20-80 km cloud area frequencies (dashed blue) are in good agreement with CPL 5 km cloud area frequencies (solid red), reducing this rate to 3.5% of total bins. This averaging of transparent layers does come at the cost of identifying false positives in the CALIOP coarse resolution results (i.e., at 20-km and 80-km). For example when averaging the 200 m CPL data to horizontal resolutions of 1 and 5 km, the cloud area frequencies over the entire CC-VEX data set increase by an average of 1.5% and 9.6%, respectively. These false positives are more significant for broken optically thin cirrus. For example the 31 July case yielded 3.4% higher cloud area frequencies at 1 km and 11.3% higher cloud area frequencies at 5 km. For optically thick homogeneous cirrus, as observed in the 11 August case, cloud area frequencies are 1.6% higher at 1 km and 2.3% higher at 5 km.

[27] Statistics of all cloud layers above 8 km for any time of day are reported in Figure 12, as well as in Tables 3, 4, and 5. For bins above 13 km, CALIOP 1 and 5 km cloud area frequencies are lower than CPL 1 and 5 km cloud area frequencies because the lower SNR of the CALIOP instruments inhibits detection of optically thin cirrus clouds in
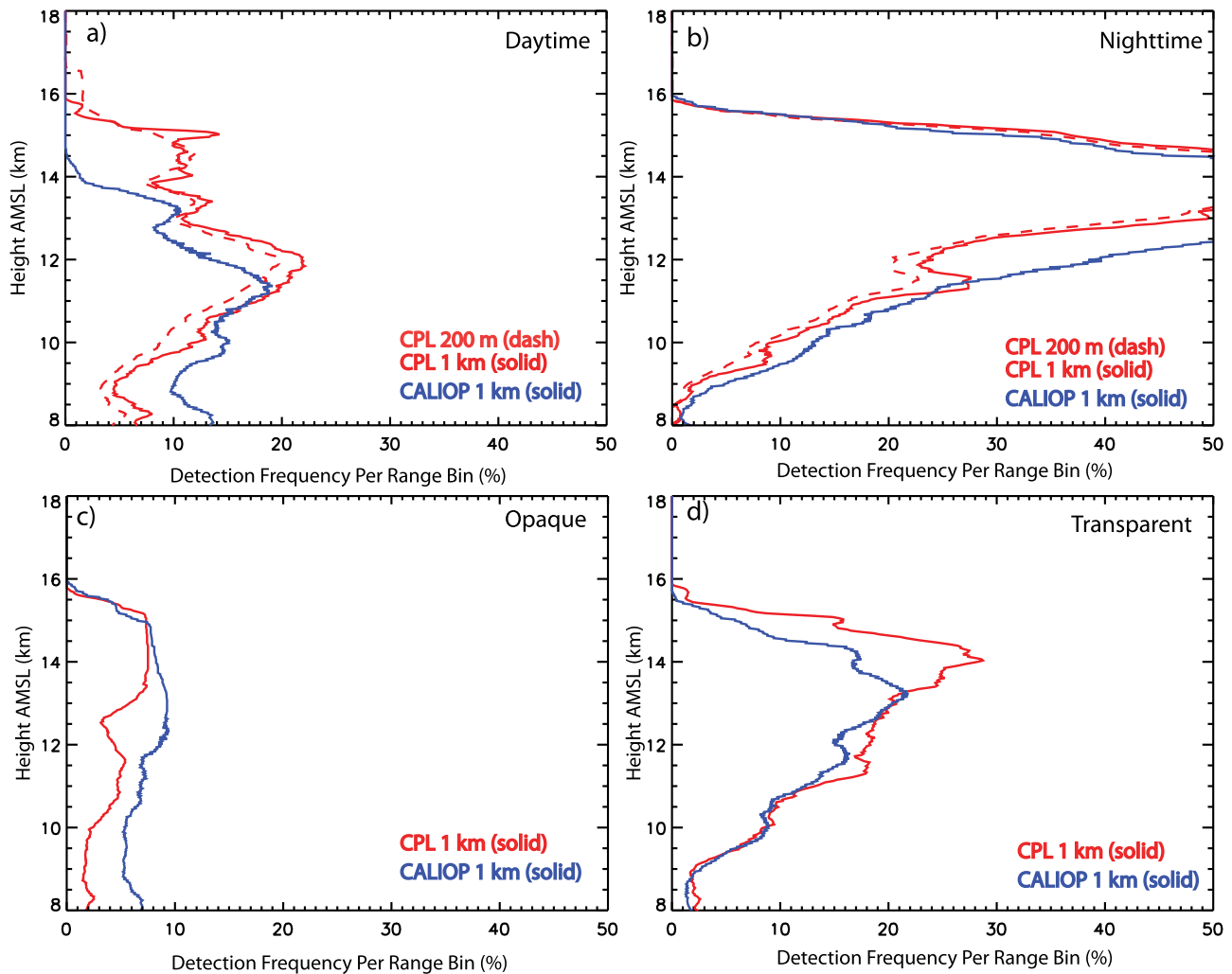
Figure 11. Cloud area detection frequency per range bin from CPL and CALIOP for all coincident overpasses during the CC-VEX project are plotted with altitude for (a) daytime, (b) nighttime, (c) opaque cloud layers, and (d) transparent cloud layers for horizontal resolutions of 200 m and 1 km. The CPL 200 m (dashed red) and 1 km (solid red) frequencies are compared to the 1 km (solid blue) CALIOP frequencies.

comparison to CPL. CPL detects a cloud where CALIPSO does not detect a cloud in 4.6% of total bins at a horizontal resolution of 5 km (Table 3). Figure 13 shows a histogram of CPL 5 km extinction values for the optically thin clouds detected by CPL but not detected by CALIOP 5 km data during daytime conditions. The extinction values of these cirrus range from less than 0.001 km^{-1} to about 8.0 km^{-1}, with a mode of 0.01 km^{-1}. Since cirrus clouds of this magnitude are important to the Earth's radiation budget, the CALIOP layer detection algorithm uses horizontal resolutions of 5-20-80 km to overcome this SNR limitation, which reduces the aforementioned percentage to 2.8%, but not without the caveat of possibly over-estimating cloud area as demonstrated in Figure 12a. CALIOP detects a cloud when CPL does not detect a cloud in 4.0% and 5.7% of total bins at spatial resolutions of 1 and 5 km, respectively. Furthermore, CALIOP 1 and 5 km cloud area frequencies are higher than CPL 1 and 5 km cloud area frequencies for bins below 13 km. These differences can be attributed to three phenomena. Multiple scattering effects in the CALIOP signal

from opaque clouds, when neither instrument is measuring the true cloud base, occur in about 2.8% of total 5 km bins sampled. Differences in the layer detection algorithms of the two instruments such as the "closing gaps between features" technique account for about 0.9% of total 5 km bins sampled. Also, other false positives, possibly caused by different cloud scenes, consist of 1.9% of total 5 km bins. Overall, CPL and CALIOP are in agreement for about 90% of total bins (clear and cloudy) for 1 and 5 km horizontal resolutions.

6. Conclusion

[28] The CPL provides "satellite-like" measurements with higher SNR, higher resolution (both vertical and horizontal) and lower multiple scattering than CALIOP, making it arguably the most comprehensive validation tool for CALIOP cirrus data products. CPL was a payload on the ER-2 aircraft that conducted flights as part of CC-VEX from 26 July to 14 August 2006. A total of ten ER-2 flights were conducted to validate the CALIPSO measurements with collocated
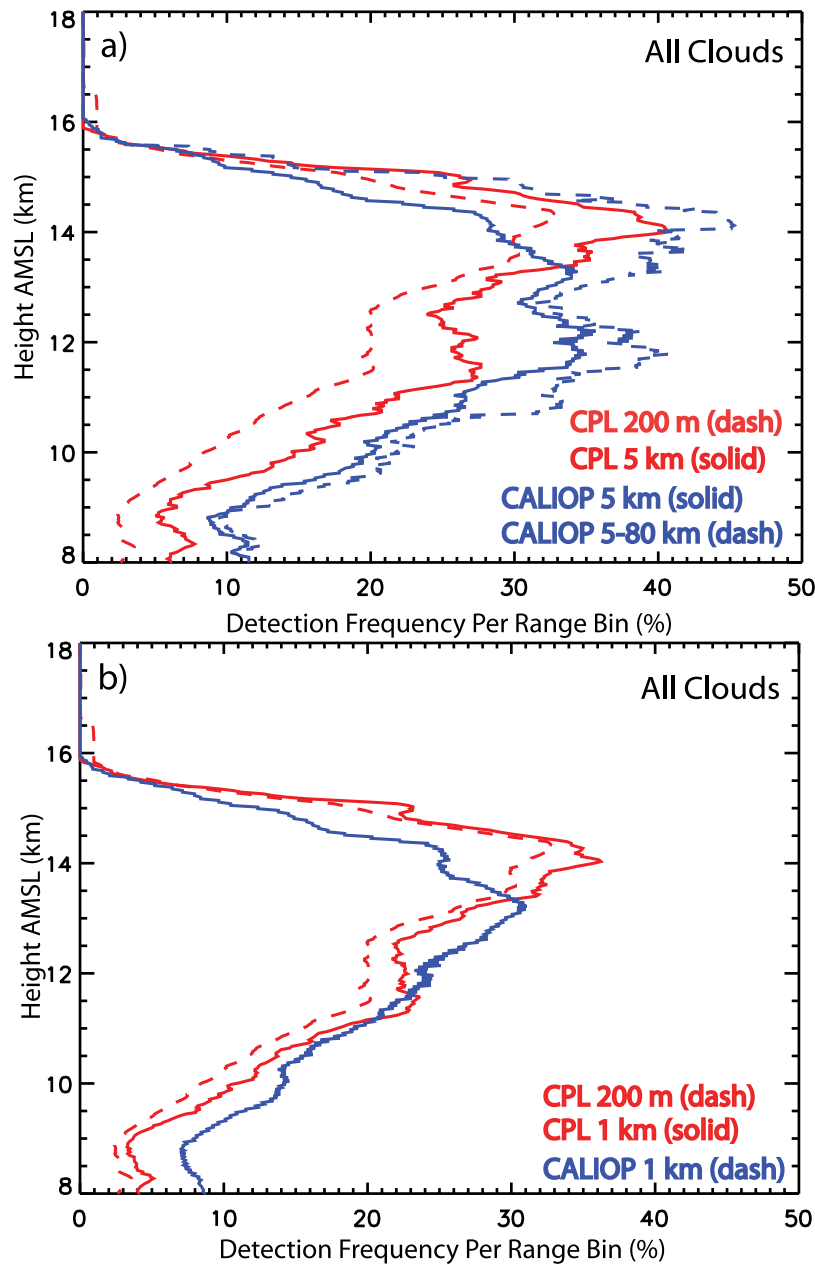
Figure 12. Cloud area detection frequency per range bin from CPL and CALIOP for all coincident overpasses during the CC-VEX project are plotted with altitude for horizontal resolutions of (a) 5 km and (b) 1 km.

data. In this study, we analyze the spatial properties of ice clouds from the 1 km and 5 km version 3 level 2 CALIPSO cloud layer products to determine how the CALIPSO data products perform in comparison with CPL cirrus detection, identify the differences between the cirrus cloud area retrieved by the two instruments, and assess the frequency and origin of these differences.

[29] Overall, there is good agreement between both instruments for cirrus cloud layer detection. CPL and CALIOP are in agreement for about 90% of total bins (clear and cloudy) for 1 and 5 km horizontal resolutions. During the nighttime hours when the SNR of both instruments is highest, CALIOP detects a cloudy bin at horizontal

resolutions of 5-20-80 km in 94.1% of bins in which CPL detects a cloudy bins at a horizontal resolution of 5 km. However, there are situations in which the two instruments do not agree on cloud layer location. The lower SNR of the CALIOP instrument occasionally inhibits detection of optically thin cirrus clouds in comparison to CPL, especially during daytime hours. CPL detects a cloud where CALIPSO does not detect a cloud in 6.1% of total daytime bins at a horizontal resolution of 5 km. This SNR limitation is improved by using the CALIOP 5-20-80 km data for layer detection, which reduces this percentage to 3.9% of total daytime bins, but not without the caveat of occasionally falsely increasing the horizontal cloud area. Instances in
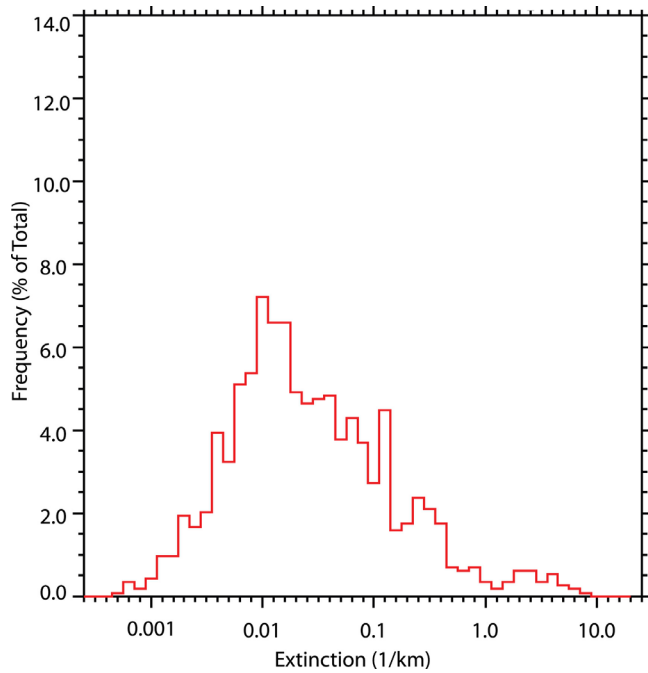
Figure 13. A histogram of CPL extinction (km^{-1}) at a horizontal resolution of 5 km for the cirrus clouds detected by CPL but not detected by CALIOP 5 km data during daytime conditions (daytime "CPL in, CALIOP out" category of Table 3).

which CALIOP detects a cloud and CPL does not detect a cloud occur in 5.7% of total bins at a spatial resolution of 5 km. This is attributed to multiple scattering effects in the CALIOP signal and differences in the layer detection algorithms of the two instruments. Uncertainties in the assumption that the instruments are observing the same cloud scene also influence the statistics. Reliable layer detection in the standard data products of both instruments is essential for the accurate derivation of layer optical properties, as well as the application of physical and optical properties resolved by the lidar systems.

References

Ackerman, S. A., R. E. Holz, R. Frey, E. W. Eloranta, B. C. Maddux, and M. McGill (2008), Cloud detection with MODIS. Part II: Validation, *J. Atmos. Oceanic Technol.*, 25, 1073–1086, doi:10.1175/2007JTECHA1053.1.

Ahlgrimm, M., and M. Köhler (2010), Evaluation of trade cumulus in the ECMWF model with observations from CALIPSO, *Mon. Weather Rev.*, 138, 3071–3083, doi:10.1175/2010MWR3320.1.

Bucholtz, A., D. L. Hlavka, M. J. McGill, K. S. Schmidt, P. Pilewskie, S. M. Davis, E. A. Reid, and A. L. Walker (2010), Directly measured heating rates of a tropical subvisible cirrus cloud, *J. Geophys. Res.*, 115, D00J09, doi:10.1029/2009JD013128.

Chand, D., R. Wood, T. L. Anderson, S. K. Satheesh, and R. J. Charlson (2009), Satellite-derived direct radiative effect of aerosols dependent on cloud cover, *Nat. Geosci.*, 2, 181–184, doi:10.1038/ngeo437.

Chepfer, H., S. Bony, D. Winker, G. Cesana, J. L. Dufresne, P. Minnis, C. J. Stubenrauch, and S. Zeng (2010), The GCM Oriented CALIPSO Cloud Product (CALIPSO-GOCCP), *J. Geophys. Res.*, 115, D00H16, doi:10.1029/2009JD012251.

Costantino, L., and F.-M. Bréon (2010), Analysis of aerosol-cloud interaction from multi-sensor satellite observations, *Geophys. Res. Lett.*, 37, L11801, doi:10.1029/2009GL041828.

Davis, S., et al. (2010), In situ and lidar observations of tropopause subvisible cirrus clouds during TC4, *J. Geophys. Res.*, 115, D00J17, doi:10.1029/2009JD013093.

Eloranta, E. W. (1998), Practical model for the calculation of multiply scattered lidar returns, *Appl. Opt.*, 37, 2464–2472, doi:10.1364/AO.37.002464.

Haladay, T., and G. Stephens (2009), Characteristics of tropical thin cirrus clouds deduced from joint CloudSat and CALIPSO observations, *J. Geophys. Res.*, 114, D00A25, doi:10.1029/2008JD010675.

Hu, Y., et al. (2007), Global statistics of liquid water content and effective number concentration of water clouds over ocean derived from combined CALIPSO and MODIS measurements, *Atmos. Chem. Phys.*, 7, 3353–3359, doi:10.5194/acp-7-3353-2007.

Hu, Y., et al. (2009), CALIPSO/CALIOP cloud phase discrimination algorithm, *J. Atmos. Oceanic Technol.*, 26, 2293–2309, doi:10.1175/2009JTECHA1280.1.

Hunt, W. H., D. M. Winker, M. A. Vaughan, K. A. Powell, P. L. Lucker, and C. Weimer (2009), CALIPSO lidar description and performance assessment, *J. Atmos. Oceanic Technol.*, 26, 1214–1228, doi:10.1175/2009JTECHA1223.1.

King, M., J. Closs, S. Spangler, R. Greenstone, S. Wharton, and M. Myers (2004), *EOS Data Products Handbook*, vol. 1, 260 pp., EOS Proj. Sci. Off., NASA Goddard Space Flight Center, Greenbelt, Md. [Available at http://eospso.gsfc.nasa.gov/ftp_docs/data_products_1.pdf.]

Li, L., G. M. Heymsfield, P. E. Racette, L. Tian, and E. Zenker (2004), A 94 GHz cloud radar system on NASA high-altitude ER-2 aircraft, *J. Atmos. Oceanic Technol.*, 21, 1378–1388, doi:10.1175/1520-0426(2004)021<1378:AGCRSO>2.0.CO;2.

Liu, Z., M. A. Vaughan, D. M. Winker, C. A. Hostetler, L. R. Poole, D. Hlavka, W. Hart, and M. McGill (2004), Use of probability distribution functions for discriminating between cloud and aerosol in lidar backscatter data, *J. Geophys. Res.*, 109, D15202, doi:10.1029/2004JD004732.

Liu, Z., et al. (2009), The CALIPSO lidar cloud and aerosol discrimination: Version 2 algorithm and initial assessment of performance, *J. Atmos. Oceanic Technol.*, 26, 1198–1213, doi:10.1175/2009JTECHA1229.1.

Mace, G. G., Q. Zhang, M. Vaughn, R. Marchand, G. Stephens, C. Trepte, and D. Winker (2009), A description of hydrometeor layer occurrence statistics derived from the first year of merged CloudSat and CALIPSO data, *J. Geophys. Res.*, 114, D00A26, doi:10.1029/2007JD009755.

McCubbin, I. B., et al. (2006), Overview of the multi-aircraft CALIPSO-CloudSAT validation experiment, *Eos Trans. AGU*, 87(52), Fall Meet. Suppl., Abstract A51E–0146.

McGill, M. J., D. L. Hlavka, W. D. Hart, V. S. Scott, J. D. Spinhirne, and B. Schmid (2002), The Cloud Physics Lidar: Instrument description and initial measurement results, *Appl. Opt.*, 41, 3725–3734, doi:10.1364/AO.41.003725.

McGill, M. J., D. L. Hlavka, W. D. Hart, E. J. Welton, and J. R. Campbell (2003), Airborne lidar measurements of aerosol optical properties during SAFARI-2000, *J. Geophys. Res.*, 108(D13), 8493, doi:10.1029/2002JD002370.

McGill, M. J., M. A. Vaughan, C. R. Trepte, W. D. Hart, D. L. Hlavka, D. M. Winker, and R. Kuehn (2007), Airborne validation of spatial properties measured by the CALIPSO lidar, *J. Geophys. Res.*, 112, D20201, doi:10.1029/2007JD008768.

Naud, C. M., A. D. Del Genio, M. Bauer, and W. Kovari (2010), Cloud vertical distribution across warm and cold fronts in CloudSat-CALIPSO data and a general circulation model, *J. Clim.*, 23, 3397–3415, doi:10.1175/2010JCLI3282.1.

Omar, A. H., J.-G. Won, D. M. Winker, S.-C. Yoon, O. Dubovik, and M. P. McCormick (2005), Development of global aerosol models using cluster analysis of Aerosol Robotic Network (AERONET) measurements, *J. Geophys. Res.*, 110, D10S14, doi:10.1029/2004JD004874.

Omar, A. H., et al. (2009), The CALIPSO automated aerosol classification and lidar ratio selection algorithm, *J. Atmos. Oceanic Technol.*, 26, 1994–2014, doi:10.1175/2009JTECHA1231.1.

Palm, S., W. Hart, D. Hlavka, E. J. Welton, A. Mahesh, and J. Spinhirne (2002), GLAS atmospheric data products: NASA Goddard Space Flight Center Geoscience Laser Altimeter System algorithm theoretical basis document version 4.2, report, 141 pp., NASA Goddard Space Flight Cent., Greenbelt, Md. [Available at http://www.csr.utexas.edu/glas/pdf/glasatmos.atbdv4.2.pdf.]

Platt, C. M. R. (1981), Remote sounding of high clouds. III: Monte Carlo calculations of multiple-scattered lidar returns, *J. Atmos. Sci.*, 38, 156–167, doi:10.1175/1520-0469(1981)038<0156:RSOHCI>2.0.CO;2.

Powell, K. A., et al. (2009), CALIPSO lidar calibration algorithms. Part I: Nighttime 532-nm parallel channel and 532-nm perpendicular channel, *J. Atmos. Oceanic Technol.*, *26*, 2015–2033, doi:10.1175/2009JTECHA1242.1.

Sassen, K., Z. Wang, and D. Liu (2008), The global distribution of cirrus clouds from CloudSat/CALIPSO measurements, *J. Geophys. Res.*, *113*, D00A12, doi:10.1029/2008JD009972.

Stephens, G. L., et al. (2002), The CloudSat mission and the A-Train: A new dimension of space-based observations of clouds and precipitation, *Bull. Am. Meteorol. Soc.*, *83*, 1771–1790, doi:10.1175/BAMS-83-12-1771.

Vaughan, M. A., S. Young, D. Winker, K. Powell, A. Omar, Z. Liu, Y. Hu, and C. Hostetler (2004), Fully automated analysis of space-based lidar data: An overview of the CALIPSO retrieval algorithms and data products, *Proc. SPIE Int. Soc. Opt. Eng.*, *5575*, 16–30, doi:10.1117/12.572024.

Vaughan, M. A., D. M. Winker, and K. A. Powell (2005), CALIOP algorithm theoretical basis document: Part 2: Feature detection and layer properties algorithms, *PC-SCI-202.01*, 87 pp., NASA Langley Res. Cent., Hampton, Va. [Available at http://www-calipso.larc.nasa.gov/resources/pdfs/PC-SCI-202_Part2_rev1x01.pdf.]

Vaughan, M., K. Powell, R. Kuehn, S. Young, D. Winker, C. Hostetler, W. Hunt, Z. Liu, M. McGill, and B. Getzewich (2009), Fully automated detection of cloud and aerosol layers in the CALIPSO lidar measurements, *J. Atmos. Oceanic Technol.*, *26*, 2034–2050, doi:10.1175/2009JTECHA1228.1.

Winker, D. M. (2003), Accounting for multiple scattering in retrievals from space lidar, in *Lidar Scattering Experiments*, edited by C. Werner, U. Oppel, and T. Rother, *Proc. SPIE Int. Soc. Opt. Eng.*, *5059*, 128–139.

Winker, D. M., B. H. Hunt, and M. J. McGill (2007), Initial performance assessment of CALIOP, *Geophys. Res. Lett.*, *34*, L19803, doi:10.1029/2007GL030135.

Winker, D. M., M. A. Vaughan, A. Omar, Y. Hu, K. A. Powell, Z. Liu, W. H. Hunt, and S. A. Young (2009), Overview of the CALIPSO mission and CALIOP data processing algorithms, *J. Atmos. Oceanic Technol.*, *26*, 2310–2323, doi:10.1175/2009JTECHA1281.1.

Yorks, J. E., M. McGill, S. Rodier, M. Vaughan, Y. Hu, and D. Hlavka (2009), Radiative effects of African dust and smoke observed from Clouds and the Earth's Radiant Energy System (CERES) and Cloud-Aerosol Lidar with Orthogonal Polarization (CALIOP) data, *J. Geophys. Res.*, *114*, D00H04, doi:10.1029/2009JD012000.

Young, S. A., and M. A. Vaughan (2009), The retrieval of profiles of particulate extinction from Cloud Aerosol Lidar Infrared Pathfinder Satellite Observations (CALIPSO) data: Algorithm description, *J. Atmos. Oceanic Technol.*, *26*, 1105–1119, doi:10.1175/2008JTECHA1221.1.

W. D. Hart, D. L. Hlavka, M. J. McGill, and J. E. Yorks, NASA Goddard Space Flight Center, Code 613.1, Greenbelt, MD 20771, USA. (john.e.yorks@nasa.gov)

R. Kuehn, Cooperative Institute for Meteorological Satellite Studies, University of Wisconsin-Madison, 1225 W. Dayton St., Madison, WI 53706, USA.

S. Rodier and M. A. Vaughan, NASA Langley Research Center, Hampton, VA 23681-2199, USA.